J. Cell. Mol. Med. Vol 15, No 5, 2011 pp. 1122-1135

Design of novel artemisinin-like derivatives with cytotoxic and anti-angiogenic properties

Shahid Soomro [a], Tobias Langenberg [b], Anne Mahringer [c], V. Badireenath Konkimalla [d], Cindy Horwedel [d], Pavlo Holenya [d], Almut Brand [d], Canan Cetin [d], Gert Fricker [c], Mieke Dewerchin [b], Peter Carmeliet [b], Edward M. Conway [e], Herwig Jansen [a], Thomas Efferth [f, *]

[a] *Dafra Pharma Research & Development, Slachthuisstraat, Turnhout, Belgium*
[b] *KU Leuven, VIB Vesalius Research Center, Herestraat, Leuven, Belgium*
[c] *Institute for Pharmacy and Molecular Biotechnology, University of Heidelberg, Im Neuenheimer Feld, Heidelberg, Germany*
[d] *German Cancer Research Center, Pharmaceutical Biology, Im Neuenheimer Feld, Heidelberg, Germany*
[e] *Centre for Blood Research, Department of Medicine, University of British Columbia, Vancouver, BC, Canada*
[f] *Department of Pharmaceutical Biology, Institute of Pharmacy and Biochemistry, University of Mainz, Mainz, Germany*

Received: October 10, 2009; Accepted: April 28, 2010

Abstract

Artemisinins are plant products with a wide range of medicinal applications. Most prominently, artesunate is a well tolerated and effective drug for treating malaria, but is also active against several protozoal and schistosomal infections, and additionally exhibits anti-angiogenic, anti-tumorigenic and anti-viral properties. The array of activities of the artemisinins, and the recent emergence of malaria resistance to artesunate, prompted us to synthesize and evaluate several novel artemisinin-like derivatives. Sixteen distinct derivatives were therefore synthesized and the *in vitro* cytotoxic effects of each were tested with different cell lines. The *in vivo* anti-angiogenic properties were evaluated using a zebrafish embryo model. We herein report the identification of several novel artemisinin-like compounds that are easily synthesized, stable at room temperature, may overcome drug-resistance pathways and are more active *in vitro* and *in vivo* than the commonly used artesunate. These promising findings raise the hopes of identifying safer and more effective strategies to treat a range of infections and cancer.

Keywords: malaria • cancer • drug resistance • P-glycoprotein • chemotherapy

Introduction

Artemisinin is a natural product of the plant *Artemisia annua L*. Reduction of artemisinin yields the more active dihydroartemisinin (DHA), a compound which is thermally less stable [1]. DHA can be further converted to different derivatives, including, for example, artesunate and artemether, which are generally referred to as artemisinins. Artemisinins are widely known for their potent anti-malarial activity [2], but also have efficacy in the treatment of several protozoal and schistosomal infections [3, 4]. Indeed, artemisinin-like compounds exhibit a wide spectrum of biological activities, including, for example, anti-angiogenic, anti-tumorigenic and even anti-viral, all of which are medically relevant [5–11].

Insights into the mechanisms of action of artemisinins are increasingly being gained. The anti-tumorigenic activity of the drug is believed to be partly due to iron-dependent generation of reactive oxygen species (ROS) [8], as well as alkylation of proteins and DNA [12, 13]. The underlying molecular mechanisms by which artemisinins suppress angiogenesis, which in turn, likely contributes to the anti-tumour activities, are less clear. Nonetheless, direct effects on angiogenesis and lymphangiogenesis have been described. Artemisinins inhibit endothelial cell proliferation, cell migration and endothelial tube formation, at least partly by inducing apoptosis. They also interfere with synthesis of

*Correspondence to: Thomas EFFERTH,
Department of Pharmaceutical Biology,
Institute of Pharmacy and Biochemistry,
University of Mainz, Staudinger Weg 5,
55128 Mainz, Germany.
Tel.: 49-6131-39-25751
Fax: 49-6131-39-23752
E-mail: efferth@uni-mainz.de

doi:10.1111/j.1582-4934.2010.01120.x

© 2011 The Authors
Journal of Cellular and Molecular Medicine © 2011 Foundation for Cellular and Molecular Medicine/Blackwell Publishing Ltd

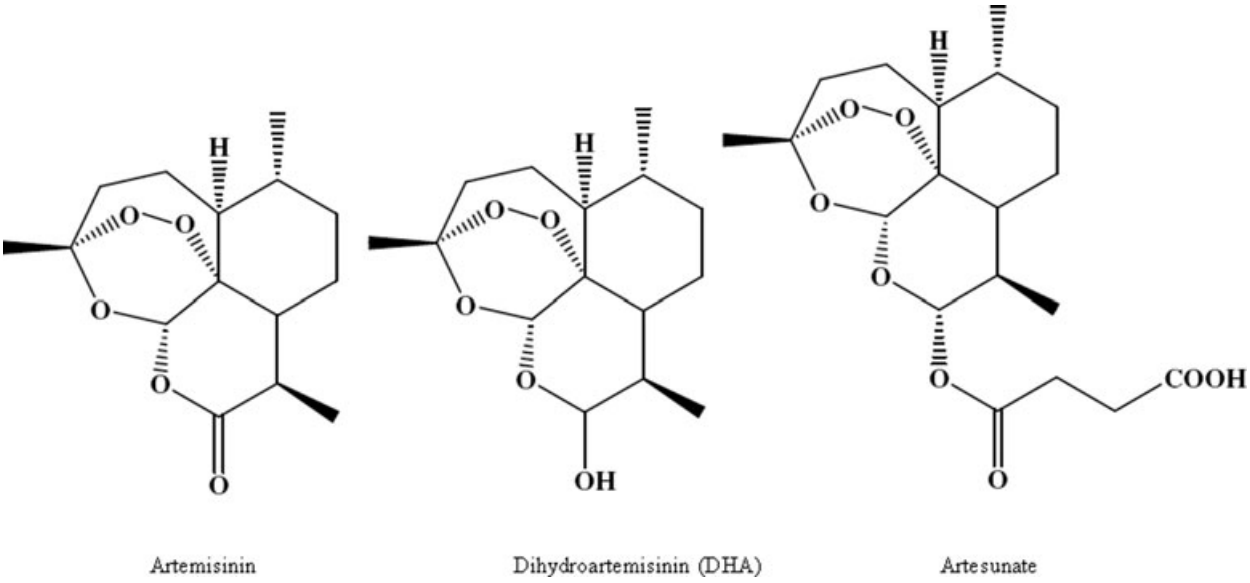

Fig. 1 Structure of artemisinin, DHA and artesunate.

vascular endothelial growth factors [14–22], possibly *via* suppression of hypoxia inducible factor activation [23].

In spite of its therapeutic utility in treating malaria, resistant strains of the malaria parasites are emerging, mostly in western Cambodia, where treatment failure rates after combination therapy have exceeded 10% [24]. The mechanisms of resistance are largely unknown, but may replicate some of those that become active in cancer cells as they develop chemoresistance. These include, among others, mutations in target proteins, resistance to apoptosis and increased drug efflux *via* transporters [25]. Interestingly, the latter mechanism is known to be used by parasites to enhance the clearance of drugs, and the multidrug resistance-conferring ATP-binding cassette (ABC) transporter, P-glycoprotein (P-gp) [26] has been implicated. Increased expression of ABC transporters such as P-gp may also enable tumour endothelial cells to escape from anti-angiogenic treatment. Because artemisinin-like compounds are generally well tolerated, with potentially wide clinical applications beyond malaria, it is important to identify alternative forms that do not induce host resistance.

In this report, we synthesized several novel artemisinin-like compounds, and tested their *in vitro* cytotoxic effects, their capacity to alter P-gp function and finally their *in vivo* anti-angiogenic properties. Our strategy was based on the generally accepted concept that DHA, a breakdown product of artesunate (see structures, Fig. 1), provides the biological activity of all the artemisinin-related compounds. Our biochemical approach was feasible, because the lactol of DHA can be converted to different derivatives, such as ethers and esters, allowing us to synthesize a range of different DHA derivatives. The findings provide new insights that will hopefully lead to the development of more effective treatment options for a variety of diseases.

Material and methods

Chemistry

Materials and reagents were purchased from Acros Organics (Beerse, Belgium) or Aldrich (Taufkirchen, Germany). Tris-(2-aminoethyl)-amine polystyrene resin was obtained from Nova biochem (Merck, Darmstadt, Germany). Nuclear magnetic resonance (NMR) spectra were recorded on a Bruker Avance DRX-400 spectrometer (400 MHz) (Bruker Daltonik, Bremen, Germany). Coupling constants (*J*) are reported in Hz. Column chromatography was performed on a Flashmaster II (Jones Chromatography) with Isolute columns pre-packed with silica gel (30e90 mM) for normal phase chromatography. Melting points were determined with a capillary melting point apparatus (Büchi 510, BUCHI, Flawil, Switzerland) and are uncorrected. Electrospray ionization mass spectra were acquired on an ion trap mass spectrometer (Bruker Daltonics esquire 3000 plus, Bruker Daltonik). LC-MS spectra were recorded on an Agilent 1100 Series HPLC system (Agilent Technologies, Böblingen, Germany) equipped with a HILIC Silica column (2.1 100 mm, 5 mm, Atlantis HILIC) (Waters, Eschborn, Germany) coupled with a Bruker Daltonics esquire 3000 plus mass spectrometer (solvent A: H_2O with 0.1% formic acid, solvent B: acetonitrile (ACN) with 0.1% formic acid, gradient 2: 90% B to 40% B, 12 min., 0.2 ml/min.). Analytical TLC was done on pre-coated silica gel plates (60 F254, 0.2 mm thick, VWR International, Darmstadt, Germany), visualization of the plates was accomplished using UV light and/or iodine staining. The dried solvents were purchased from Acros Organics. Artemisinin, DHA and artesunate were provided by Dafra Pharma R&D (Turnhout, Belgium), anhydrodihydroartemisinin (4) [27], deoxoartemisinin (3) [28], 10-dihydroartemisinyl acetate (7) [29], compound 5a synthesized by a modified procedure, $NaOH/H_2O_2$ were used as oxidizing agents [30], 10-dihydroartemisinyl benzoate [13, (29) with small modification, instead of benzoylchloride, the benzoic anhydride was used with catalytic amount of 4-(dimethylamino)-pyridine (DMAP)] were prepared as previously described.

© 2011 The Authors

Journal of Cellular and Molecular Medicine © 2011 Foundation for Cellular and Molecular Medicine/Blackwell Publishing Ltd

Synthesis of 10-dihydroartemisinyl 2′, 2′-dichloroacetate (8)

DMAP (0.6 g, 4.9 mmol) and dichloroacetic anhydride (6.0 g, 25 mmol) were added to a stirred solution of DHA (5 g, 17.6 mmol) in dichloromethane (300 ml) at 0°C and the reaction mixture was slowly brought to room temperature and stirred for 6 hrs, during which time, all DHA was consumed. The solvent was removed under reduced pressure and the residue was purified by flash chromatography with ethyl acetate/hexane (10:90 to 50:50) to provide the product dense liquid (3.82 g, 55%). ^{1}H-nuclear magnet resonance (HNMR) (400, $CDCl_3$) d 0.86 (d, $J = 7.0$ Hz, 3 H, 9-Me), 0.97 (d, $J = 5.95$ Hz, 20 3 H, 6-Me), 1.45 (s, 3 H, 3-Me), 1.23–1.94 (m, 9 H), 2.04 (ddd, $J = 14.5, 5.0, 3.0$ Hz, 1 H), 2.39 (ddd, $J = 14.5$, 5.0, 3.0 Hz, 1H), 2.55 (m, 1 H, H-9), 5.40 (s, 1 H, H-12), 5.90 (d, $J = 10.0$ Hz, 1H, H-10), 6.25 (s, 1H, $COCHCl_2$); electron ionization mass spectrometry (EIMS) (m/z) 396.3 $(M+H)^+$.

Synthesis of 10-dihydroartemisinyl butyrate (9)

DMAP (0.6 g, 4.9 mmol) and butyric anhydride (4.0 g, 25 mmol) were added to a stirred solution of DHA (5 g, 17.6 mmol) in dichloromethane (300 ml) at 0°C and the reaction mixture was slowly brought to room temperature and stirred for 8 hrs, during which time, all DHA was consumed. The solvent was removed under reduced pressure and the residue was purified by flash chromatography with ethyl acetate/hexane (10:90 to 50:50). Re-crystallization from ethyl acetate/hexane provided white big crystals (5.9 g, 95%), m. p. 81–85°C. ^{1}HNMR (400, $CDCl_3$) d 0.86 (d, $J = 7.0$ Hz, 3 H, 9-Me), 0.97 (d, $J = 5.95$ Hz, 3 H, 6-Me), 1.17–1.24 (m, 6 H), 1.45 (s, 3 H, 3-Me), 1.23–1.94 (m, 9 H), 2.04 (ddd, $J = 14.5, 5.0, 3.0$ Hz, 1 H), 2.39 (ddd, $J = 14.5, 5.0$, 15 3.0 Hz, 1H), 2.55 (m, 1 H, H-9), 2.68 (m, 1 H, COCH), 5.45 (s, 1 H, H-12), 5.850 (d, $J = 10.0$ Hz, 1 H, H-10); EIMS (m/z) 355.4 $(M+H)^+$.

10-dihydroartemisinyl propionate and butyrate are similar. ^{1}HNMR of 10-dihydroartemisinyl propionate ^{1}HNMR (400, $CDCl_3$) d 0.91 (d, $J = 7.0$ Hz, 3 H, 9-Me), 1.03 (d, $J = 5.95$ Hz, 3 H, 6-Me), 1.17–1.24 (m, 6 H), 1.50 (s, 3 H, 3-Me), 1.23–1.94 (m, 7 H), 2.04 (ddd, $J = 14.5, 5.0, 3.0$ Hz, 1 H), 2.39 (ddd, $J = 14.5, 5.0$, 15 3.0 Hz, 1H), 2.55 (m, 1 H, H-9), 2.68 (m, 1 H), 5.51 (s, 1 H, H-12), 5.87 (d, $J = 10.0$ Hz, 1 H, H-10).; EIMS (m/z) 350.0 $(M+H)^+$.

Synthesis of 10-dihydroartemisinyl ^{i}butyrate (10)

DMAP (0.6 g, 4.9 mmol) and isobutyric anhydride (4.0 g, 25 mmol) were added to a stirred solution of DHA (5 g, 17.6 mmol) in dichloromethane (200 ml) at 0°C and the reaction mixture was slowly brought to room temperature and stirred for 8 hrs, during which time, all DHA was consumed. The solvent was removed under reduced pressure and the residue was purified by flash chromatography with ethyl acetate/hexane (10:90 to 50:50) to provide the product dense liquid (5.2 g, 84%). ^{1}HNMR (400, $CDCl_3$) d 0.86 (d, $J = 7.0$ Hz, 3 H, 9-Me), 0.97 (d, $J = 5.95$ Hz, 3 H, 6-Me), 1.17–1.24 (m, 6 H) 1.45 (s, 3 H, 3-Me), 1.23–1.94 (m, 9 H), 2.04 (ddd, $J = 14.5, 5.0, 3.0$ Hz, 1 H), 2.39 (ddd, $J = 14.5, 5.0$, 15 3.0 Hz, 1H), 2.55 (m, 1 H, H-9), 2.68 (m, 1 H, COCH), 5.45 (s, 1 H, H-12), 5.850 (d, $J = 10.0$ Hz, 1 H, H-10); EIMS (m/z) 355.4 $(M+H)^+$.

Synthesis of 10-dihydroartemisinyl 2′-propylpentanoate (11)

DMAP (0.5 g, 4.1 mmol) and triethylamine (3.03 g, 30 mmol) were added to a stirred solution of DHA (7.1 g, 25 mmol) in dichloromethane (400 ml). 2-Proplypentanlychloride (4.87 g, 30 mmol) at −30°C was added, and the reaction mixture was continuously stirred for 2 hrs and slowly brought to room temperature and stirred overnight. The solvent was removed under reduced pressure and the residue was purified by flash chromatography with ethyl acetate/hexane (10:90 to 50:50) to provide the product as a white solid. Re-crystallization from ethyl acetate/hexane resulted in a colourless liquid (8.19 g, 80%). ^{1}HNMR (400, $CDCl_3$) d 0.86 (d, $J = 7.0$ Hz, 3 H, 9-Me), 0.90 (t, 6H), 0.97 (d, $J = 5.95$ Hz, 3 H, 6-Me), 1.33 (m, 4H), 1.45 (s, 3 H, 3-Me), 1.64 (m, 4H), 1.23–1.94 (m, 9 H), 2.04 (ddd, $J = 14.5, 5.0, 3.0$ Hz, 1 H), 2.29 (t, 1 H), 2.39 (ddd, $J = 14.5, 5.0$, 15 3.0 Hz, 1H), 2.55 (m, 1 H, H-9), 5.45 (s, 1 H, H-12), 5.850 (d, $J = 10.0$ Hz, 1H, H-10); EIMS (m/z) 411.5 $(M+H)^+$.

Synthesis of 10-dihydroartemisinyl 2′, 2′-dimethylpropianate (12)

DMAP (0.5 g, 4.1 mmol) and trimethylacetic anhydride (5.59 g, 30 mmol) were added to a stirred solution of DHA (7.1 g, 25 mmol) in dichloromethane (400 ml) at 0°C. The reaction mixture was slowly brought to room temperature and stirred overnight, during which time all DHA was consumed. The crude material was washed with water (2 × 100 ml), and the solvent was removed under reduced pressure. The product was then re-crystallized from ethyl acetate/hexane, yielding white crystals (5.17 g, 75%), m. p. 101–104°C. ^{1}HNMR (400, $CDCl_3$) d 0.86 (d, $J = 7.0$ Hz, 3 H, 9-Me), 0.97 (d, $J = 5.95$ Hz, 3 H, 6-Me), 1.25 (s, 9H $C(CH)_3$), 1.45 (s, 3 H, 3-Me), 1.23–1.94 (m, 9 H), 2.04 (ddd, $J = 14.5, 5.0, 3.0$ Hz, 1 H), 2.39 (ddd, $J = 14.5, 5.0$, 15 3.0 Hz, 1H), 2.55 (m, 1 H, H-9), 5.45 (s, 1 H, H-12), 5.850 (d, $J = 10.0$ Hz, 1H, H-10); EIMS (m/z) 369.5 $(M+H)^+$.

Synthesis of 10-dihydroartemisinyl N′, N′-dimethylacetamide (14)

DMAP (0.5 g, 4.1 mmol) and dimethylcarbomoyl chloride (3.23 g, 30 mmol) were added to a stirred solution of DHA (7.1 g, 25 mmol) in dichloromethane (400 ml) at 0°C. The reaction mixture was slowly brought to room temperature and stirred for 8 hrs, during which time all DHA was consumed. The crude material was washed with water (2 × 100 ml) and the solvent was removed under reduced pressure. The residue was purified by flash chromatography with ethyl acetate/hexane (10:90 to 90:10), yielding a white dense liquid (5.8 g, 65%). ^{1}HNMR (400, $CDCl_3$) d 0.86 (d, $J = 7.0$ Hz, 3 H, 9-Me), 0.97 (d, $J = 5.95$ Hz, 3 H, 6-Me), 1.45 (s, 3 H, 3-Me), 1.23–1.94 (m, 9 H), 2.04 (ddd, $J = 14.5, 5.0, 3.0$ Hz, 1 H), 2.39 (ddd, $J = 14.5, 5.0$, 15 3.0 Hz, 1H), 2.55 (m, 1 H, H-9), 2.92 (s, 3H, $N(\underline{CH_3})_2$, 2.98 (s, 3H, $N(\underline{CH_3})_2$, 5.45 (s, 1 H, H-12), 5.68 (d, $J = 10.0$ Hz, 1H, H-10); EIMS (m/z) 356.4 $(M+H)^+$.

Synthesis of 10-(2′-butyloxy) dihydroartemisinin (15)

Boron trifluoride-diethyl ether (3 ml) was added to a stirred solution of DHA (1, 2.56 g, 9.0 mmol) and ^{i}butanol (2.2 g, 30 mmol) in diethyl ether (100 ml). After 6 hrs, the reaction mixture was quenched with saturated aqueous $NaHCO_3$ and dried with $MgSO_4$. Filtration and concentration of the

© 2011 The Authors
Journal of Cellular and Molecular Medicine © 2011 Foundation for Cellular and Molecular Medicine/Blackwell Publishing Ltd

filtrate gave a residue which on flash chromatography with ethyl acetate/hexane (5:95 to 10:90), yielded a white microcrystalline powder (2.05 g, 67%), m.p. 100–101°C. ^{1}HNMR (400, $CDCl_3$) d 0.86 (d, $J = 7.0$ Hz, 3 H, 9-Me), 0.97 (d, $J = 5.95$ Hz, 3 H, 6-Me), 1.08 (d, $J = 6.1$Hz, 3H), 1.20 (d, $J = 6.2$ Hz, 3H), 1.45 (s, 3 H, 3-Me), 1.23–1.94 (m, 9 H), 2.04 (ddd, $J = 14.5, 5.0, 3.0$ Hz, 1 H), 2.39 (ddd, $J = 14.5, 5.0, 15$ 3.0 Hz, 1H), 2.55 (m, 1 H, H-9), 4.0 (m, 1 H, $OCH(CH_3)_2$), 4.87 (d, $J = 3.5$ Hz, 1 H, H-10), 5.44 (s, 1 H, H-12); EIMS (m/z) 341.5 $(M+H)^+$.

Synthesis of 10-dihydroartemisinyl thioethylamine (16)

DHA (7.1 g, 25 mmol) and cysteamine (2.7 g, 35 mmol) were dissolved in 300 ml dichloromethane and boron trifluoride-diethyl ether (10 ml) was added slowly at 0°C. The reaction mixture was stirred for 3 hrs at 0°C and an additional 1 hr at room temperature. The reaction was quenched with 5% $NaHCO_3$ and extracted with dichloromethane. The solvent was removed under reduced pressure and the residue was purified by flash chromatography with ethyl acetate/hexane (10:90) to yield a brown wax product (4.7 g, 55%). ^{1}HNMR (400, $CDCl_3$) d 0.86 (d, $J = 7.0$ Hz, 3 H, 9-Me), 0.97 (d, $J = 5.95$ Hz, 3 H, 6-Me), 1.25, 1.45 (s, 3 H, 3-Me), 1.23–1.94 (m, 9 H), 2.04 (ddd, $J = 14.5, 5.0, 3.0$ Hz, 1 H), 2.39 (ddd, $J = 14.5, 5.0$, 15 3.0 Hz, 1 H), 2.55 (m, 1 H, H-9), 2.9 (t, 2H), 3.1 (t, 2H), 4.56 (d, $J = 10.0$ Hz, 1 H, H-10), 5.31 (s, 1 H, H-12); EIMS (m/z) 344.5 $(M+H)^+$.

XTT cytotoxicity assay

Multidrug-resistant, P-gp-overexpressing CEM/ADR5000 cells and their parental, drug-sensitive counterpart, CCRF-CEM cells were used. The cell lines were provided by Dr. Daniel Steinbach (University of Ulm, Ulm, Germany). Doxorubicin resistance of CEM/ADR5000 was maintained as described [31]. CEM/ADR5000 cells have previously been shown to selectively express multidrug resistance (MDR)1 (ABCB1), but none of the other ABC transporters [32]. The cell lines were maintained in Roswell Park Memorial Institute (RPMI) medium (Life Technologies, Carlsbad, CA, USA) supplemented with 10% foetal calf serum in a humidified 7% CO_2 atmosphere at 37°C. Cells were passaged twice weekly. All experiments were done with cells in the logarithmic growth.

Cytotoxicity was assessed using the 2,3-bis[2-methoxy-4-nitro-5-sulfophenyl]-2H-tetrazolium-5-carboxanilide inner salt (XTT) assay kit (Roche, Indianapolis, IN, USA), which measures the metabolic activity of viable cells [33, 34]. Toxicity of compounds was determined with the Cell Proliferation Kit II (Roche Diagnostics, Mannheim, Germany), according to the manufacturer's instructions. Fresh stock solutions of each compound were prepared in dimethyl sulfoxide (DMSO) at a concentration of 100 mM, and a dilution series was prepared in Dulbecco's minimal essential medium (DMEM). Cells were suspended at a final concentration of 1×10^5 cells/ml, and 100 ml were aliquoted per well into a 96-well culture plate (Costar Corning, Lowell, MA, USA). Marginal wells were filled with 100 μl of media to minimize evaporation. A row of wells with cells was left untreated and another row of wells with cells was treated with 1 μl DMSO, the latter serving as a solvent control. All studies were performed in duplicate, in a range of concentrations and in two independent experiments with different batches of cells. Quantification of cytotoxicity was achieved with an ELISA plate reader (Bio-Rad, München, Germany) at 490 nm with a reference wavelength of 655 nm, and reported as a percentage of viability compared to untreated cells. The ligand binding module of Sigma plot software (version 10.0) was used for analysis.

HUVEC proliferation/viability assay

Single donor human umbilical vein endothelial cells (HUVECs) cells were purchased from Lonza (Breda, Netherlands). Cells were seeded at 5000 cells per well in 96-well microtitre plates in endothelial cell growth medium (EGM)-2EV medium (Invitrogen, Darmstadt, Germany). Upon adherence the cells were gently washed twice with phosphate-buffered solution and starved overnight in EGM-2EV medium with reduced foetal bovin serum (FBS) content (0.1%; starvation medium). The medium was then aspirated and replaced with starvation medium with or without 30 ng/ml recombinant human vascular endothelial growth factor (VEGF)165 (R&D System, Wiesbaden, Germanys) and with or without increasing concentrations of compound 1 (artemisinin), 7 and 10 (0.5–100 μM). Due to its precipitation from the cell culture medium, artesunate could not be used as a reference compound. After 96 hrs, cell growth was quantified using the water-soluble tetrazolinum (WST)1 Rapid cell proliferation kit (Calbiochem, Merck, Darmstadt, Germany), and was expressed in percentage of the control value (VEGF alone). Experiments were carried out in triplets.

Isolation of porcine brain capillary endothelial cells (PBCECs)

PBCECs were isolated from porcine brains as reported [35]. Briefly, freshly isolated porcine brains were collected from the local slaughterhouse, cleaned of meninges, choroid plexus and superficial blood vessels. After removal of grey matter, the tissue was minced into cubes <2 mm^3 and incubated in Medium 199, supplemented with 0.8 mM L-glutamine, penicillin/streptomycin (100 U/ml), 100 μg/ml gentamicin and 10 mM 2-(4-(2-hydroxyethyl)-1-piperazinyl)-ethane sulfonic acid (HEPES), pH 7.4 (Biochrom, Berlin, Germany) with dispase II (0.5%) (Roche Diagnostics) for 2 hrs at 37°C. After centrifugation at $1000 \times g$ for 10 min. at 4°C, the supernatant was discarded and the pellet was re-suspended in media containing 15% dextran (Sigma-Aldrich, Taufkirchen, Germany). Micro-vessels were separated by centrifugation at $5800 \times g$ for 15 min. at 4°C and incubated in 20 ml medium containing collagenase–dispase II (1 mg/ml) (Roche Diagnostics) for 1.5–2 hrs at 37°C. The resulting cell suspension was filtered through a 150 μm Polymon® mesh (NeoLab Migge, Heidelberg, Germany) and centrifuged for 10 min. at $130 \times g$ at 4°C. The cell pellet was re-suspended in media containing 9% horse serum (Biochrom) and separated on a discontinuous Percoll (Sigma-Aldrich) gradient consisting of Percoll® 1.03 g/ml (20 ml) and 1.07 g/ml (15 ml) by centrifugation at $1000 \times g$ for 10 min. at 4°C. Endothelial cells were enriched at the interface between the two Percoll solutions. Cells were collected, washed in media with 9% horse serum at 4°C, and stored with 10% DMSO in liquid nitrogen until use.

Calcein–AM assay

Freshly isolated or recently thawed PBCECs were incubated in DMEM/HAM's F12 1:1 (Biochrom) for 1 hr at 37°C at a cell density of 2.5×10^6 cells/10 ml. Test compounds were dissolved in DMSO as stock solutions and further dilutions were made with DMEM/Ham's F12 1:1 (Biochrom). DMSO concentration in the cell suspension did not exceed 1%, a concentration that was determined not to affect the assay. A range of concentrations of test compound in a volume of 300–600 μl cell suspension were added, followed by a 15 min. incubation at 37°C. Calcein–acetoxymethyl ester (AM) (300 μl) (MoBiTec, Göttingen, Germany) in DMEM/HAM's F12 1:1 was added to a final concentration of

© 2011 The Authors

Journal of Cellular and Molecular Medicine © 2011 Foundation for Cellular and Molecular Medicine/Blackwell Publishing Ltd

1 μM and incubated for 30 min. at 37°C. Suspensions were then centrifuged at 200 × *g* for 5 min. cells were washed with 4°C DMEM/HAM's F12 1:1, and centrifuged again at 200 × *g* for 5 min. at 4°C. The supernatant was discarded and cells were lysed with 600 μl 1% Triton X100 for 10 min. on ice. 100 μl of clarified cell lysate was added to 1 well of a 96-well microplate. Fluorescence was detected with a Fluoroskan Ascent plate reader (Labsystems, Helsinki, Finland) (l [excitation] = 485 nm and l [emission] = 520 nm). All concentrations and controls were measured 10–12 times, at least three experiments were performed per test compound.

Flow cytometry

For the calcein–AM assay using flow cytometry, the cell density of suspensions in DMEM/Ham's F12 1:1 was 2.5×10^7 cells/ml. Intracellular fluorescence was measured using a fluorescence-activated cell sorting system (FACS: Calibur flow cytometer, Becton-Dickinson, Franklin Lakes, NJ, USA) with l (excitation) = 488 nm and a 530/30 band-pass filter to collect emitted fluorescence. Gating on forward and side scatter in concert with propidium iodide staining allowed us to distinguish live endothelial cells. Twenty thousand cells were sorted in each run, and data were processed and analysed with CellQuest (Franklin Lakes, NJ, USA). All fluorescence signals were corrected for background fluorescence. Calcein–AM autohydrolysis was measured in control samples ($n = 6$) without cells. The increase in intracellular fluorescence induced by a test compound was compared to control fluorescence levels (100%), and results are reported as percentage of control.

In vivo experiments

Tg(fli1:EGFP) zebrafish, which express enhanced green fluorescent protein (GFP) in their endothelial cells, were used as an *in vivo* model for angiogenesis [36]. At 20 hrs after fertilization (hpf), zebrafish embryos (10 per well/condition) were bathed in fish media, containing a concentration range of each of the compounds or control. Compounds had been dissolved as stock solutions in DMSO, stored at room temperature and serially diluted in fish media prior to use. The anti-angiogenic tyrosinase kinase inhibitor SU5416 (Pfizer, Berlin, Germany) [37], and a vehicle-alone control containing the maximum concentration of DMSO were used as controls in all experiments. In the first sets of experiments, a broad range of concentrations were used to identify the maximum tolerable dose, based on toxicity to the embryos, visualized directly by light microscopy. Subsequent experiments were performed a minimum of two times. Live analyses of the embryos were performed under light and fluorescence microscopy at 28 and 48 hpf to monitor viability, overall morphology and pattern of swimming. Angiogenesis was evaluated visually by fluorescence microscopy. The developmental growth and patterning of the dorsal aorta, posterior cardinal vein, intersomitic vessels (ISV) and vascular plexus were monitored, as was the heart rate and blood flow.

Results

Synthesis of compounds

To identify novel artemisinin-like compounds for evaluation of efficacy in different models, we synthesized several acetal and non-acetal derivatives of DHA. Esters (Fig. 2) were made by reacting DHA with corresponding anhydrides or acid chloride in basic medium in the presence of triethylamine, as reported [29]. The ether and amine (Fig. 3) were made by reacting DHA with a Levis acid forming an oxonium ion [38], that reacts with nucleophiles, such as alcohol or amine, and converts to ether (or amine) derivatives. In the absence of nucleophiles, it forms an anhydro product 4, or it can be further reduced in the presence of Et_3SiH to obtain the product 3. Compound 4 was further converted to alcohol 5a-b (5a major product) by addition of borane followed by hydrogen peroxide and aqueous NaOH (Fig. 4). A similar reaction was previously reported [39].

Cytotoxicity (XTT assay)

All compounds were tested both towards drug-sensitive CCRF-CEM leukaemia cells and their multidrug-resistant subline, CEM/ADR5000. The IC_{50} values are summarized in Table 1. Acetal type C-10 derivatives were more active than non-acetal derivatives 3 and 4. The degree of cross-resistance of CEM/ADR5000 cells towards the various compounds ranged from 0.06 (compound 4) to 22.46 (compound 8). Substitution played an important role in C-10 derivatives. In general, alkyl side chains showed high efficacy in terms of activity and cross-resistance when compared to aromatic side chain 13 and dichloroacetate side chain 8. Branched side chain substances possessed more activity than their straight-chain counterparts as in the case of compounds 9 and 10. When C-10 ether 15 is compared with ester 10, the activity remains the same in both cases, but ether shows slightly less drug resistance than ester.

Calcein assays

As a next step, we analysed whether the transport of calcein was affected by artemisinin and its derivatives to answer the question, whether artemisinin-like compounds act as P-gp inhibitors. As can be seen in Figure 5, the calcein fluorescence in CCRF-CEM and CEM/ADR5000 cell is low and not different in both cell lines after exposure to artemisinin or artesunate. This indicates that these two drugs do not act as P-gp inhibitors. In contrast, all other compounds tested led to an intracellular accumulation of calcein in multidrug-resistant CEM/ADR5000 cells, indicating an inhibition of the efflux activity of P-gp. Their EC50 values were in a range from 17.35 ± 1.3 μM (11) to 61.8 ± 9.62 μM (15). Intracellular calcein fluorescence increased from 916% (7) up to 3343% (14) compared to untreated controls, suggesting high affinities of these compounds to P-gp (Table 2). Well-known P-gp inhibitors were chosen as controls, *e.g.* verapamil and PSC-833 [38, 39].

Inhibition of blood brain barrier function

The inhibitory potential of artemisinin derivatives towards P-gp expressed in porcine capillaries was analysed by confocal microscopy. Figure 6 shows control capillaries, where luminal

© 2011 The Authors
Journal of Cellular and Molecular Medicine © 2011 Foundation for Cellular and Molecular Medicine/Blackwell Publishing Ltd

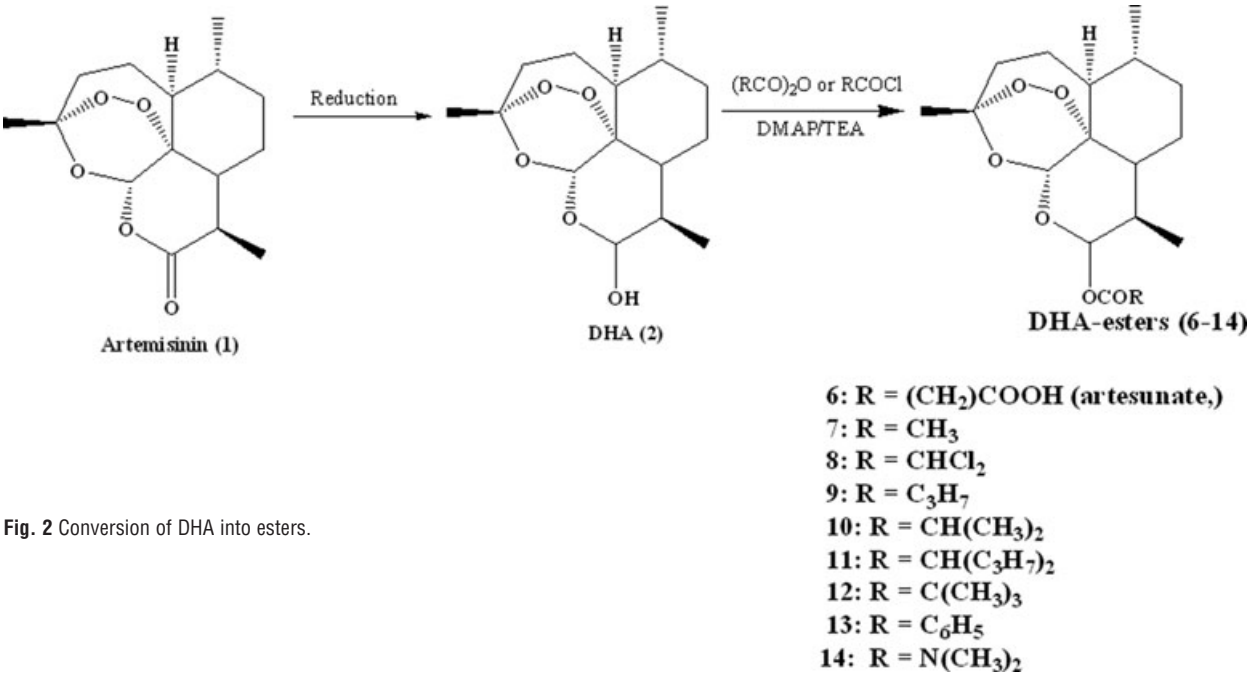

Fig. 2 Conversion of DHA into esters.

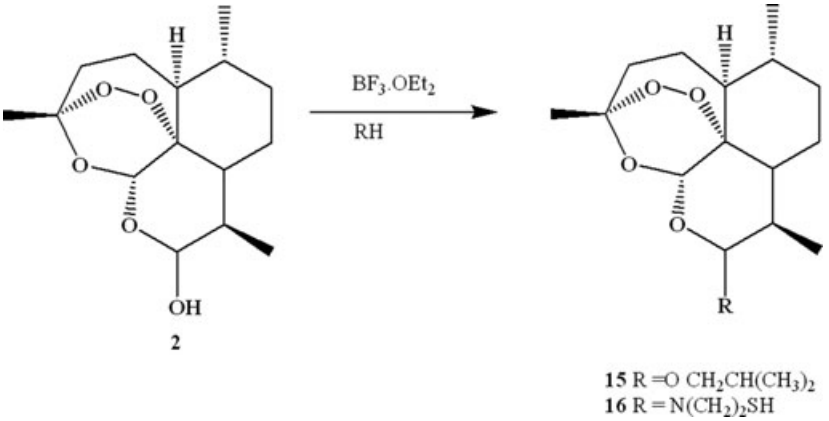

Fig. 3 Conversion of DHA into ether and amine.

localized P-gp effluxes a fluorescent P-gp substrate [40], N-ε-(4-nitrobenzofurazan-7-yl)-d-Lys8 (NBD)-cyclosporin A (NBD-CSA) back into the capillary lumen (green). Exposure to both 8 and 15 resulted in an almost empty lumen, indicating that the P-gp substrate NBD-CSA accumulated in the endothelial cells, indicating inhibition of P-gp (Fig. 6). Luminal P-gp was inhibited by a well-known selective P-gylcoprotein inhibitor, PSC-833 (data not shown) [41].

The inhibition of luminal P-gp in porcine brain capillaries by seven artemisinin derivatives was quantified by fluorospectrometry (Fig. 6, bottom row).

Inhibition of angiogenesis *in vivo*

Eight compounds (4, 7, 8, 9, 10, 11, 12 and 15) were compared to artesunate for their anti-angiogenic potential using an *in vivo* zebrafish embryo model system (Fig. 7 and Table 3). DMSO at concentrations of 0.5%, 1% and 2% were used as vehicle control. No effects were observed on overall morphology, heart rate, blood flow or angiogenesis in control embryos. The anti-angiogenic agent SU5416 was used as a positive control [37]. At a concentration of 10 μg/ml, SU5416 completely blocked formation of ISVs at 28 hpf. At 48 hpf ISVs sprouted only minimally as compared to

© 2011 The Authors

Journal of Cellular and Molecular Medicine © 2011 Foundation for Cellular and Molecular Medicine/Blackwell Publishing Ltd

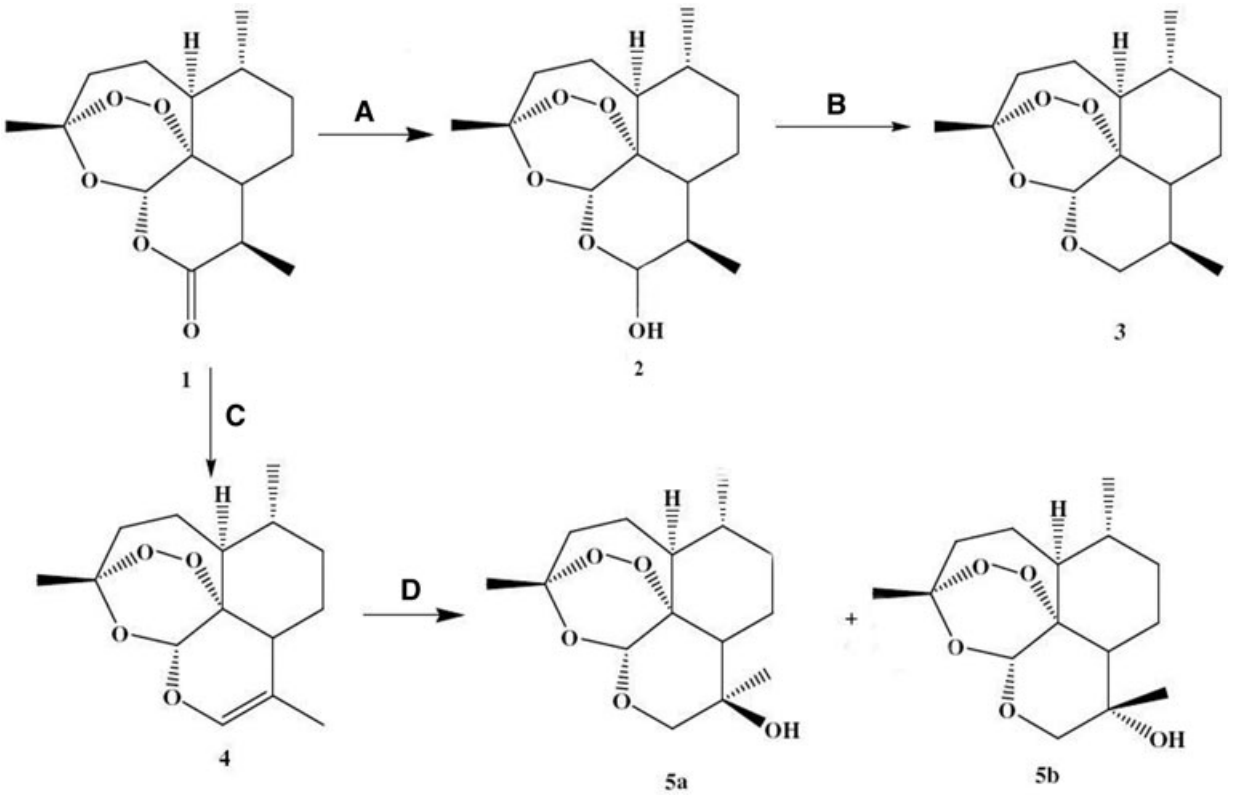

Fig. 4 Synthetic scheme of compounds 3, 4 and 5. Reagents and conditions: (**A**) $NaBH_4$, THF; (**B**) $BF_3.OEt_2/Et_3SiH$, CH_2Cl_2; (**C**) $BF_3.OEt_2$, CH_2Cl_2; (**D**) i. BH_3, THF; ii. 3 M NaOHaq, H_2O_2 30%, THF.

control embryos. The heart rate was not affected by SU5416, and oedema was rarely observed.

Of the compounds tested, 7, 8, 9, 10, 11 and artesunate exhibited dose-dependent anti-angiogenic effects. Although there was some inter-experimental variability in the dose–response, compounds 7 and 8 consistently had distinct anti-angiogenic properties. Similarly, compounds 9, 10 and 11 also suppressed angiogenesis, but there was more toxicity than with compounds 7 and 8 at higher doses. Compound 12 was the most toxic at comparable doses, and a specific anti-angiogenic effect was not observed. All of the compounds that did suppress angiogenesis were more effective, on a dose basis, than artesunate. Of note, all compounds induced bradycardia in a dose-dependent manner, and this occurred irrespective of effects on angiogenesis. Oedema, a typical consequence of heart insufficiency, coincided with the bradycardia. Preliminary experiments on rabbit hearts indicate that the bradycardia is unique to the zebrafish and not observed in mammalian models (data not shown).

Inhibition of VEGF-induced HUVEC proliferation

To further test the anti-angiogenic potential of our novel compounds, we assayed proliferation and survival of HUVECs treated with VEGF and two compounds that were very active in the zebrafish model. Artemisinin and VEGF alone served as control and reference compound (Fig. 8). In this assay, despite the presence of the proliferation-inducing VEGF, compounds 7 and 10 inhibited the proliferation and survival of HUVECs significantly stronger than artemisinin. Notably, the survival rate of HUVECs was very poor after more than 48 hrs exposure to the compounds when VEGF was omitted (data not shown).

Discussion

By synthesizing several artemisinin-like derivatives, we have identified a range of unique compounds that may ultimately be of clinical value. It is well known that C-10 derivatives of DHA can act as pro-drugs, and that the introduction of bulky substitutes at this position decreases the rate of hydrolysis beginning with the propionate and isopropionate and different substitutes. Thus the resultant compound derivatives may be released more slowly, potentially increasing the circulating half-life and possibly the therapeutic efficacy. Indeed, compound 10 is branch substituted, likely reducing the rate of hydrolysis at C-10, which may contribute to its greater cytotoxicity as compared with compound 9.

© 2011 The Authors
Journal of Cellular and Molecular Medicine © 2011 Foundation for Cellular and Molecular Medicine/Blackwell Publishing Ltd

Table 1 Cytotoxicity of artemisinin derivatives towards drug-sensitive CCRF-CEM and multidrug-resistant CEM/ADR5000 leukaemia cell lines

Compound	CCRF-CEM (μM)	CEM/ADR5000 (μM)	Degree of resistance
1	148.05 ± 16.64	94.92 ± 30.46	0.64
2	0.87 ± 0.13	1.84 ± 0.31	2.11
3	240.73 ± 50.68	117.38 ± 8.20	0.49
4	83.36 ± 7.51	33.64 ± 0.68	0.4
5a	156.15 ± 52.05	90.03 ± 4.57	0.58
6	0.55 ± 0.03	0.46 ± 0.03	0.84
7	0.18 ± 0.43	2.36 ± 0.64	12.83
8	1340.96 ± 1268.63	87.46 ± 96.84	0.06
9	106.00 ± 25.41	54.99 ± 16.00	0.51
10	12.30 ± 3.86	276.30 ± 213.41	22.46
11	2.68 ± 0.10	3.31 ± 0.24	1.23
12	6.65 ± 1.17	17.64 ± 4.56	2.65
13	171.00 ± 97.58	1333.54 ± 507.76	7.79
14	1.05 ± 0.14	20.75 ± 8.05	19.76
15	16.68 ± 7.34	7.96 ± 3.76	0.47
16	0.86 ± 0.19	3.34 ± 0.64	3.88

Table 2 EC50 and EC max values of artemisinin derivatives in the calcein-AM assay using multidrug-resistant CEM/ADR5000 cells and flow cytometry

Compound	EC50 (μM)	EC max (%)
1	n.d.	114.1 ± 2.85
2	n.d.	114.3 ± 10.19
7	50.23 ± 48.5	916 ± 829.9
8	19.47 ± 5.25	1380 ± 199.3
9	36.37 ± 13.86	1387 ± 393.8
10	26.45 ± 3.12	1240 ± 78.2
11	17.35 ± 1.3	2224 ± 94.7
12	35.0 ± 8.65	1776 ± 292.5
13	17.97 ± 5.51	2645 ± 423.6
14	27.51 ± 2.59	3343 ± 197
15	61.8 ± 9.62	1180 ± 178.7
16	27.17 ± 4.69	1011 ± 106.3

n.d.: not detectable.

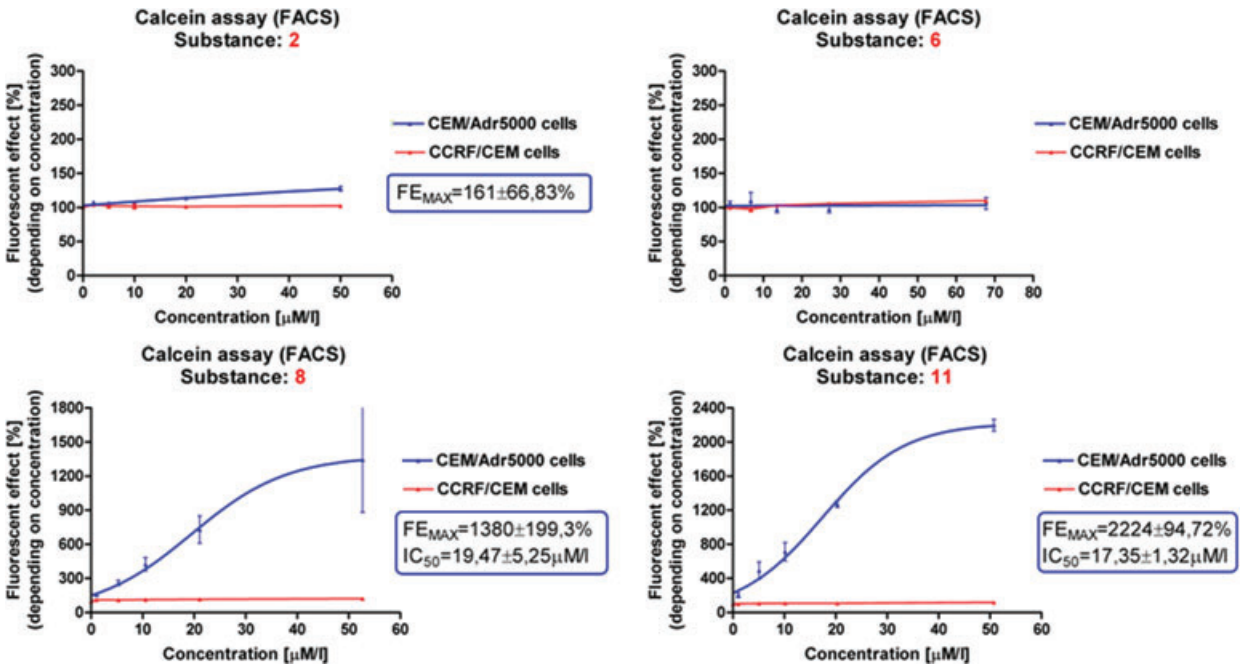

Fig. 5 Inhibition of calcein ametoxymethylester efflux from human leukaemia CCRF/CEM and CEM/Adr5000 cells by different concentrations of the testing substances – derivatives of artesunate. The intracellular accumulation of calcein inside the cells is measured by using FACS analysis. The points indicate mean values of fluorescent effect, vertical lines show standard error calculated on the base of two independent experiment replicates. The effect corresponds to a control of cells which were treated only with calcein.

© 2011 The Authors

Journal of Cellular and Molecular Medicine © 2011 Foundation for Cellular and Molecular Medicine/Blackwell Publishing Ltd

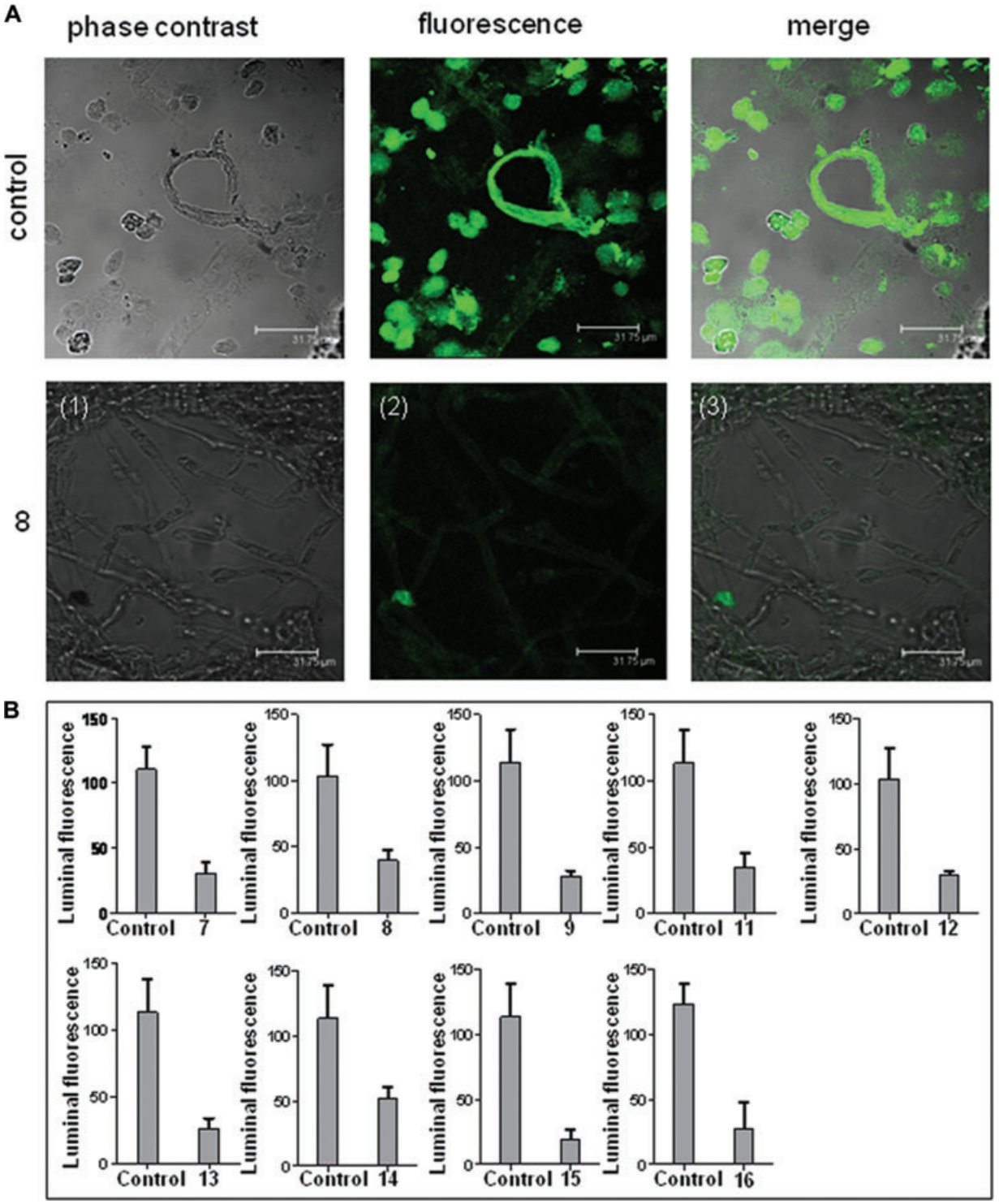

Fig. 6 (**A**) High-magnification micrographs of porcine brain capillaries incubated with substance 8. (first row) negative control (capillaries stained only with NBD-CSA in the same time course); (second row) (1) transmitted light image of several capillaries; (2) confocal fluorescent micrograph of several capillaries; in addition to the capillary endothelium, these vessels may contain pericytes within the wall of the capillary and blood cells within the lumen; (3) overlay of 1 and 2 (**B**)Transport of the P-gp substrate NBD-CSA into porcine brain capillary lumens in the absence of control and presence of testing substances.

© 2011 The Authors
Journal of Cellular and Molecular Medicine © 2011 Foundation for Cellular and Molecular Medicine/Blackwell Publishing Ltd

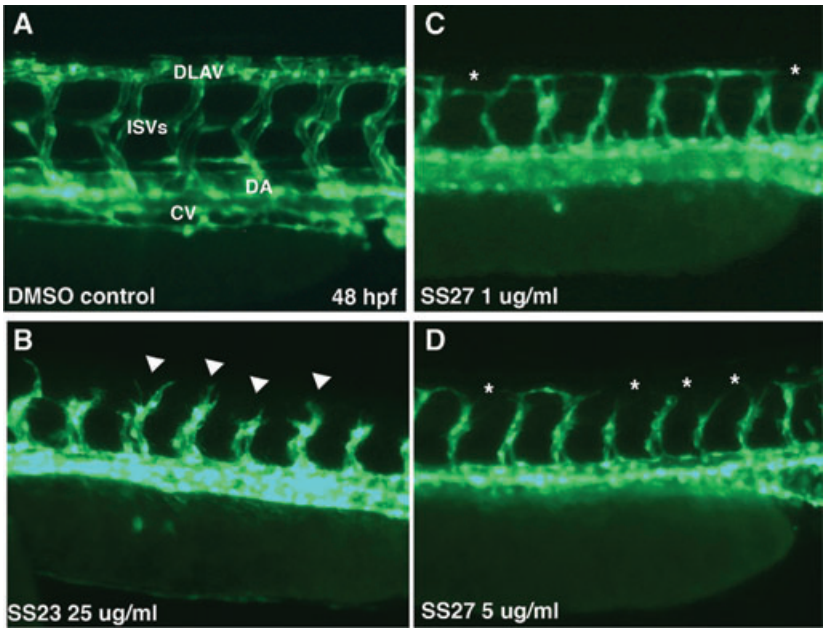

Fig. 7 Artemisinin derivatives inhibit angiogenesis *in vivo*. Lateral views of the trunk region of zebrafish embryos are shown at 48 hrs after fertilization (hpf) (head to the left) that were treated with 1% DMSO (**A**, control) or artemisinin derivatives (**B**–**D**) from 19–48 hpf. (**A**) At 48 hpf, several blood vessels can clearly be distinguished in the trunk of the embryo: dorsal aorta (DA), posterior cardinal vein (PCV), ISVs, dorsal longitudinal anastomosing vessel (DLAV). (**B**) In an embryo treated with 25 μg/ml of compound 9, the ISVs are stunted (arrowheads) and the DLAV has not formed. (**C**, **D**) Compound 11 has a dose-dependent effect on blood vessel formation. At 1 μg/ml, ISVs are thin and the DLAV is incomplete (asterisks). At the higher dose of 5 μg/ml, several ISVs are severely reduced and the DLAV has many gaps (asterisks).

Additional factors that likely impact on the activity of these compounds are solubility and conversion to DHA. In contrast to artemisinin, artesunate is water soluble and metabolized to DHA. These distinct properties may at least in part explain the greater cytotoxicity of artesunate as compared to that of artemisinin. This is exemplified by our findings that C10 derivatives, which are metabolized to DHA, were more cytotoxic towards cancer cells than C9 derivatives, which cannot be metabolized to DHA. Overall, most of the new derivatives presented in this report are not only generally more active than artemisinin, but were easily synthesized and are stable at room temperature.

In the treatment of cancer, drug resistance remains a major impediment to success. One well-characterized pathway that promotes drug resistance is the P-gp transfer system [42, 43].

Its relevance in clinical oncology is well known. For example, P-gp is expressed at the blood brain barrier, thereby hindering the delivery of functionally active anti-tumour drugs to the central nervous system [44–46].

Unfortunately, overcoming drug resistance by using compounds, such as verapamil or PSC-833 that interfere with P-gp function, has not successfully entered the clinic due to excess toxicity [47]. Notably, artemisinin and artesunate are well tolerated in clinical malaria studies [48], and we have determined that the artemisinin-like compounds that we synthesized also modulate P-gp function, as measured with the calcein assay. Thus, in combination with classical chemotherapeutic, P-glycoproptein substrates such as vinblastine, paclitaxel and other anti-tumour drugs, these novel artemisinin-like derivatives may enhance tumour cell killing, with lower toxicity, less drug resistance and improved response rates.

As the ABC transporter, P-gp, is not the only drug resistance mechanism, the question arises about the cross-resistance of artemisinin-type compounds to anticancer drugs and about the relevance of other members of the ABC transporter family. In addition to the doxorubicin-resistant P-gp overexpressing CEM/ADR5000 cell line, artemisinin and derivatives were not cross-resistant to MRP-1-overexpressing HL60 leukaemia cells and breast cancer resistance protein (BCRP)-overexpressing MDA-MB-231 breast cancer cells [10]. They do not exhibit cross-resistance in cell lines selected for vincristine or epirubicin resistance [49], nor to cell lines selected for methotrexate or hydroxyurea [9]. Furthermore, we found that cisplatin resistant ovarian carcinoma cells were also not cross-resistant to artemisinins (Sertel *et al.*, submitted for publication). There was no relationship between expression of P-gp, MRP1 and BCRP and the sensitivity or resistance to artemisinin and eight different artemisinin derivatives in 55 cell lines of different tumour types (leukaemia, colon Ca, breast Ca, lung Ca, prostate Ca, renal ca, brain cancer, ovarian Ca) [5, 9, 50, 51]. This result has been confirmed in another cell line panel with 39 cell lines of different tumour origin [52] and investigation using cell lines derived from Kaposi sarcoma [19], medularry thyroid carcinoma [53] and non-Hodgkin lymphoma [54]. All these data indicate that artemisinin-type compounds may be active in otherwise drug-resistant cancer cells.

In the present study, we found that some artemisinin derivatives exert collateral sensitivity, *i.e.* doxorubicin-resistant P-gp overexpressing CEM/ADR5000 cells were more sensitive to these compounds than the parental wild-type CCRF-CEM cells. Collateral sensitivity is a well-known phenomenon in multidrug-resistance cancer cells for more than three decades [54] and led to the development of treatment strategies with compounds that selectively kill multidrug resistant cancer cells [56, 57], although the mechanisms are still poorly understood. It has been proposed that compounds extruded by P-gp consume ATP and repletion of ATP

© 2011 The Authors

Journal of Cellular and Molecular Medicine © 2011 Foundation for Cellular and Molecular Medicine/Blackwell Publishing Ltd

Table 3 Anti-angiogenic effects in the zebrafish *in vivo* assay. *N* = total number of embryos tested (in multiples of 10); Dead = number of dead embryos up to 48 hpf; Vasc. defects = number of surviving embryos with vascular defects; Other = other defects observed: bradycardia (B) or oedema (E).

Compound	Conc. (μg/ml)	N	Dead	Vasc. defects	Other
Artesunate	25	20	1	0	B
	50	20	1	2	B, E
	100	20	1	6	B, E
	200	10	1	9	B, E
4	50	10	2	0	B
	75	10	5	0	B, E
7	0.1	10	1	1	-
	1.0	20	2	3	B, E
	10	20	3	4	B, E
	25	10	0	1	B, E
	50	20	4	8	B, E
	75	10	3	7	B, E
	100	20	4	16	B, E
8	1.0	10	0	2	-
	10	10	0	1	B
	25	10	0	10	B, E
	50	10	0	10	B, E
9	1.0	20	2	4	B
	5.0	10	2	2	B, E
	10	20	3	6	B, E
	15	10	1	9	B, E
	25	30	17	13	B, E
	50	10	5	5	B, E
10	0.5	10	2	3	B, E
	1.0	20	5	7	B, E
	10	20	5	10	B, E
11	1.0	30	3	9	B, E
	5.0	20	9	11	B, E
	10	30	22	8	B, E
12	1.0	10	0	0	B, E
	10	10	1	0	B, E
	25	10	9	0	B, E
15	1.0	10	0	0	-
	10	10	1	0	B
	25	10	0	0	B, E

from ADP by oxidative phosphorylation generates ROS [58]. ROS production may lead to increased cell killing. This view is conceivable with the fact that cell with high P-gp expression exhibit higher collateral sensitivity than cells with low P-gp levels. It is well known that Artemisinin derivatives produce ROS leading to apoptosis [59, 60]. Hence, it can be speculated that some of our derivatives produced more ROS than others leading to higher degrees of collateral sensitivity.

In addition to collateral sensitivity, the question about possible synergistic effects in combination treatments can be asked. Indeed, we previously found that the combination of artesunate increased the apoptosis-inducing effects of doxorubicin in CEM/ADR5000 leukaemia cells [59]. A comparable result has also been reported for *Plasmodium falciparum*, doxorubicin and artemisinin showed synergistic interaction as compared to each drug alone [61].

Furthermore, it should be pointed out that the CEM/ADR5000 cell line represents a suitable model for MDR analyses. We have previously shown that that this cell line selectively expresses ABCB1, but not other ABC transporters. This has been shown in a microarray-based study with a biochip carrying the genes of the ABC transporter family and validated by real-time RT-PCR [32]. Hence, the CEM/ADR5000 cell line provides a comparable genetic background as transfected cell lines do.

Although *in vitro* evidence supports the notion that several of the artemisinin-like compounds that we synthesized have potential benefits, it was important to examine their role in an *in vivo* model. Because artemisinins have been implicated in suppressing angiogenesis *via* several mechanisms, we utilized the zebrafish embryo model to directly visualize effects on vascular development. We chose the zebrafish due to the availability of a transgenic line that expresses GFP in all endothelial cells [34], which allows direct observation of blood vessel formation. Despite the seemingly distant relationship of human beings and zebrafish, there is a remarkable homology at the genetic level: most human genes have zebrafish orthologues and the zebrafish is more and more recognized as a valuable model for human diseases [62, 63].

Our findings support the hypothesis that several of the artemisin-like compounds have anti-angiogenic properties (Figs 7 and 8). For example, compounds 9 and 11 suppressed ISV formation at concentrations as low as 1 μg/ml, above which toxicity became evident. Similarly, compounds 7 and 8 also exhibited anti-angiogenic effects, with somewhat lesser toxicity. When tested in a HUVEC proliferation/survival assay, compounds 7 and 10 were more effective at inhibiting cellular proliferation than artemisinin, despite the presence of the strong proliferation inducing growth factor VEGF.

The results of the present panel of novel artemisinine derivatives are in accord with previous reports that artemisinin, DHA and artesunate act in an anti-angiogenic manner by interfering with angiogenesis-regulating genes such as vascular endothelial growth factor receptor (VEGFR), thrombopplastin, thrombospondin 1, plasminogen activator, matrix metalloproteinase 9, etc. [18–22].

Overall, our findings demonstrate that these synthesized artemisinin-like compounds are not only endowed with different

© 2011 The Authors
Journal of Cellular and Molecular Medicine © 2011 Foundation for Cellular and Molecular Medicine/Blackwell Publishing Ltd

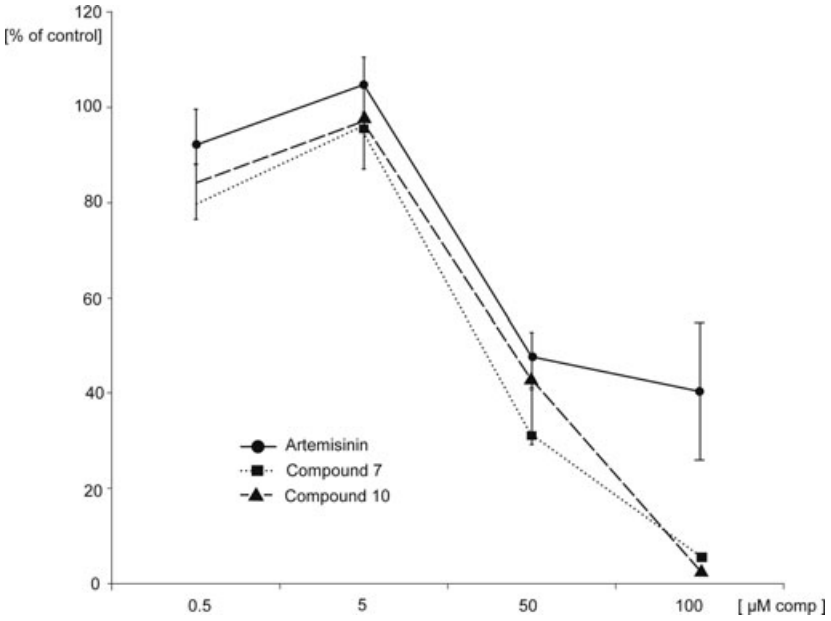

Fig. 8 Inhibition of VEGF-driven HUVEC proliferation. Optical density (OD) as a measure of viable cells at various concentrations of compounds 7, 10 and artemisinin, expressed as percentage of control (VEGF) treated HUVECs. Increasing levels of artemisinin-like compounds strongly inhibit proliferation/survival of HUVECs even in the presence of VEGF. Error bars = S.E.M.

properties in terms of stability and P-gp modulating activity, but that they retain potent *in vivo* biologic anti-angiogenic properties, that provide strong rationale for further examination of their effects in treating a range of diseases in larger animal models.

Acknowledgements

P.C. is supported by grants from 'long-term structural funding: Methusalem funding by the Flemish Government'. The authors thank Joris Souffreau for technical assistance.

References

1. **Haynes RK, Chan HW, Lung CM**, ***et al.*** Artesunate and dihydroartemisinin (DHA): unusual decomposition products formed under mild conditions and comments on the fitness of DHA as an Antimalarial drug. *Chem Med Chem*. 2007; 2: 1448–63.
2. **Jansen FH, Soomro SA**. Chemical instability determines the biological action of the artemisinins. *Curr Med Chem*. 2007; 14: 3243–59.
3. **Utzinger J, Xiao SH, Tanner M**, ***et al.*** Artemisinins for schistosomiasis and beyond. *Curr Opin Investig Drugs*. 2007; 8: 105–16.
4. **Shu-Hua X, Utzinger J, Chollet J**, ***et al.*** Effect of artemether administered alone or in combination with praziquantel to mice infected with Plasmodium berghei or Schistosoma mansoni or both. *Int J Pararasitol*. 2006; 36: 957–64.
5. **Efferth T**. Mechanistic perspectives for 1, 2, 4-trioxanes in anti-cancer therapy. *Drug Resist Update*. 2005; 8: 85–97.
6. **Efferth T**. Willmar Schwabe Award 2006: antiplasmodial and antitumor activity of artemisinin–from bench to bedside. *Planta Med*. 2007; 73: 299–309.
7. **Golenser J, Waknine JH, Krugliak M**, ***et al.*** Current perspectives on the mechanism of action of artemisinins. *Int J Parasitol*. 2006; 36: 1427–41.
8. **Nakase I, Lai H, Singh NP**, ***et al.*** Anticancer properties of artemisinin derivatives and their targeted delivery by transferrin conjugation. *Int J Pharm*. 2008; 354: 28–33.
9. **Efferth T, Dunstan H, Sauerbrey A**, ***et al.*** The anti-malarial artesunate is also active against cancer. *Int J Oncol*. 2001; 18: 767–73.
10. **Efferth T, Sauerbrey A, Olbrich A**, ***et al.*** Molecular modes of action of artesunate in tumor cell lines. *Mol Pharmacol*. 2003; 64: 382–94.
11. **Efferth T, Romero MR, Wolf DG**, ***et al.*** The antiviral activities of artemisinin and artesunate. *Clin Infect Dis*. 2008; 47: 804–11.
12. **Jefford CW**. Why artemisinin and certain synthetic peroxides are potent antimalarials. Implications for the mode of action. *Curr Med Chem*. 2001; 8: 1803–26.
13. **Haynes RK, Chan WC, Lung CM**, ***et al.*** The Fe2+-mediated decomposition, PfATP6 binding, and antimalarial activities of artemisone and other artemisinins: the unlikelihood of C-centered radicals as bioactive intermediates. *Chem Med Chem*. 2007; 2: 1480–97.
14. **Chen HH, Zhou HJ, Wu GD**, ***et al.*** Inhibitory effects of artesunate on angiogenesis and on expressions of vascular endothelial growth factor and VEGF receptor KDR/flk-1. *Pharmacology*. 2004; 71: 1–9.
15. **Chen HH, Zhou HJ, Fang X**. Inhibition of human cancer cell line growth and human umbilical vein endothelial cell angiogenesis by artemisinin derivatives *in vitro*. *Pharmacol Res*. 2003; 48: 231–6.

© 2011 The Authors

Journal of Cellular and Molecular Medicine © 2011 Foundation for Cellular and Molecular Medicine/Blackwell Publishing Ltd

16. **Wang J, Guo Y, Zhang BC**, ***et al.*** Induction of apoptosis and inhibition of cell migration and tube-like formation by dihydroartemisinin in murine lymphatic endothelial cells. *Pharmacology*. 2007; 80: 207–18.
17. **Wang J, Zhang B, Guo Y**, ***et al.*** Artemisinin inhibits tumor lymphangiogenesis by suppression of vascular endothelial growth factor C. *Pharmacology*. 2008; 82: 148–55.
18. **Zhou HJ, Wang WQ, Wu GD**, ***et al.*** Artesunate inhibits angiogenesis and downregulates vascular endothelial growth factor expression in chronic myeloid leukemia K562 cells. *Vascul Pharmacol*. 2007; 47: 131–8.
19. **Dell'Eva R, Pfeffer U, Vene R**, ***et al.*** Inhibition of angiogenesis *in vivo* and growth of Kaposi's sarcoma xenograft tumors by the anti-malarial artesunate. *Biochem Pharmacol*. 2004; 68: 2359–66.
20. **Anfosso L, Efferth T, Albini A**, ***et al.*** Microarray expression profiles of angiogenesis-related genes predict tumor cell response to artemisinins. *Pharmacogenomics J*. 2006; 6: 269–78.
21. **Huan-huan C, Li-Li Y, Shang-Bin L**. Artesunate reduces chicken chorioallantoic membrane neovascularisation and exhibits antiangiogenic and apoptotic activity on human microvascular dermal endothelial cell. *Cancer Lett*. 2004; 211: 163–73.
22. **Chen HH, Zhou HJ, Wang WQ**, ***et al.*** Antimalarial dihydroartemisinin also inhibits angiogenesis. *Cancer Chemother Pharmacol*. 2004; 53: 423–32.
23. **Huang XJ, Ma ZQ, Zhang WP**, ***et al.*** Dihydroartemisinin exerts cytotoxic effects and inhibits hypoxia inducible factor-1alpha activation in C6 glioma cells. *J Pharm Pharmacol*. 2007; 59: 849–56.
24. **White NJ**. Qinghaosu (artemisinin): the price of success. *Science*. 2008; 320: 330–4.
25. **Broxterman HJ, Lankelma J, Hoekman K**. Resistance to cytotoxic and anti-angiogenic anticancer agents: similarities and differences. *Drug Resist Update*. 2003; 6: 111–27.
26. **Duraisingh MT, Cowman AF**. Contribution of the pfmdr1 gene to antimalarial drug-resistance. *Acta Trop*. 2005; 94: 181–90.
27. **Haynes RK, Chan HW, Cheung MK**, ***et al.*** Stereoselective preparation of 10alpha-and 10beta-aryl derivatives of dihydroartemisinin. *Eur J Org Chem*. 2003; 2098–114.
28. **Avery MA, Mehrotra S, Johnson TL**, ***et al.*** Structure activity relationships of the antimalarial agent artemisinin. 5. Analogs of 10-deoxoartemisinin substituted at C-3 and C-9. *J Med Chem*. 1996; 39: 4149–55.
29. **Haynes RK, Chan HW, Cheung MK**, ***et al.*** C-10 ester and ether derivatives of dihydroartemisinin- 10-a artesunate, preparation of authentic 10-ß artesunate, and of other ester and ether derivatives bearing potential aromatic intercalating groups at C-10. *Eur J Org Chem*. 2002; 113–32.
30. **Jung M, Lee K, Jung H**. First synthesis of (+)-deoxoartemisitene and its novel C-11 derivatives. *Tetrahedron Lett*. 2001; 42: 3997–4000.
31. **Kimmig A, Gekeler V, Neumann M**, ***et al.*** Susceptibility of multidrug-resistant human leukemia cell lines to human interleukin 2-activated killer cells. *Cancer Res*. 1990; 50: 6793–9.
32. **Gillet JP, Efferth T, Steinbach D**, ***et al.*** Microarray-based detection of multidrug resistance in human tumor cells by expression profiling of ATP-binding cassette transporter genes. *Cancer Res*. 2004; 64: 8987–93.
33. **Scudiero DA**. Evaluation of a soluble tetrazolium/formazan assay for cell growth and drug sensitivity in culture using human and other tumor cell lines. *Cancer Res*. 1988; 48: 4827–33.
34. **Konkimalla BV, Blunder M, Korn B**, ***et al.*** Effect of artemisinins and other endoperoxides on nitric oxide-related signaling pathway in RAW 264.7 mouse macrophage cells. *Nitric Oxide*. 2008; 19: 184–91.
35. **Huwyler J, Drewe J, Klusemann C, Fricker G**. Evidence for P-glycoprotein-modulated penetration of morphine-6-glucuronide into brain capillary endothelium. *Br J Pharmacol*. 1996; 118: 1879–85.
36. **Lawson ND, Weinstein BM**. *In vivo* imaging of embryonic vascular development using transgenic zebrafish. *Dev Biol*. 2002; 248: 307–18.
37. **Parng C, Seng WL, Semino C**, ***et al.*** Zebrafish: a preclinical model for drug screening. *Assay Drug Dev Technol*. 2002; 1: 41–8.
38. **Jung M, Lee K, Kim H**, ***et al.*** Recent advances in artemisinin and its derivatives as antimalarial and antitumor agents. *Curr Med Chem*. 2004; 11: 1265–84.
39. **Clark SJ, Kettle JG**. Synthesis of sub-units of marine polycyclic ethers by ring-closing metathesis and hydroboration of enol ethers. *Tetrahedron*. 1999; 55: 8231–48.
40. **Schramm U, Fricker G, Wenger R**, ***et al.*** P-glycoprotein-mediated secretion of a fluorescent cyclosporin analogue by teleost renal proximal tubules. *Am J Physiol Renal Physiol*. 1995; 268: 46–52.
41. **Twentyman PR, Bleehen NM**. Resistance modification by PSC-833, a novel non-immunosuppressive cyclosporin [corrected]. *Eur J Cancer*. 1991; 27: 1639–42.
42. **Efferth T**. The human ATP-binding cassette transporter genes: from the bench to the bedside. *Curr Mol Med*. 2001; 1: 45–65.
43. **Gillet JP, Efferth T, Remacle J**. Chemotherapy-induced resistance by ATP-binding cassette transporter genes. *BBA-Rev Cancer*. 2007; 1775: 237–62.
44. **Adams M, Mahringer A, Kunert O**, ***et al.*** Cytotoxicity and p-glycoprotein modulating effects of quinolones and indoloquinazolines from the Chinese herb Evodia rutaecarpa. *Planta Med*. 2007; 73: 1554.
45. **Adams M, Mahringer A, Bauer R**, ***et al.*** *In vitro* cytotoxicity and P-glycoprotein modulating effects of geranylated furocoumarins from Tetradium daniellii. *Planta Med*. 2007; 73: 1475.
46. **Fricker G**. Drug interactions with natural products at the blood brain barrier. *Curr Drug Metab*. 2008; 9: 1019–26.
47. **Tan B, Piwnica-Worms D, Ratner L**. Multidrug resistance transporters and modulation. *Curr Opin Oncol*. 2000; 12: 450–8.
48. **Ribeiro IR, Olliaro P**. Safety of artemisinin and its derivatives. A review of published and unpublished clinical trials. *Med Trop*. 1998; 58: 50–3.
49. **Efferth T, Davey M, Olbrich A**, ***et al.*** Activity of drugs from traditional Chinese medicine toward sensitive and MDR1- or MRP1-overexpressing multidrug-resistant human CCRF-CEM leukemia cells. *Blood Cells Mol Dis*. 2002; 28: 160–8.
50. **Efferth T, Olbrich A, Bauer R**. mRNA expression profiles for the response of human tumor cell lines to the antimalarial drugs artesunate, arteether, and artemether. *Biochem Pharmacol*. 2002; 64: 617–23.
51. **Efferth T, Oesch F**. Oxidative stress response of tumor cells: microarray-based comparison between artemisinins and anthracyclines. *Biochem Pharmacol*. 2004; 68: 3–10.
52. **Kelter G, Steinbach D, Konkimalla VB** ***et al.*** Role of transferrin receptor and the ABC transporters ABCB6 and ABCB7 for resistance and differentiation of tumor cells towards artesunate. *PLoS One*. 2007; 2: e798.
53. **Rinner B, Siegl V, Pürstner P**, ***et al.*** Activity of novel plant extracts against medullary thyroid carcinoma cells. *Anticancer Res*. 2004; 24: 495–500.

© 2011 The Authors
Journal of Cellular and Molecular Medicine © 2011 Foundation for Cellular and Molecular Medicine/Blackwell Publishing Ltd

54. **Sieber S, Gdynia G, Roth W**, ***et al.*** Combination treatment of malignant B cells using the anti-CD20 antibody rituximab and the anti-malarial artesunate. *Int J Oncol*. 2009; 35: 149–58.
55. **Bech-Hansen NT, Till JE**, ***et al.*** Pleiotropic phenotype of colchicine-resistant Chocells: cross-resistance and collateral sensitivity. *J Cell Physiol*. 1976; 88: 23–31.
56. **Szakács G, Annereau JP, Lababidi S**, ***et al.*** Predicting drug sensitivity and resistance: profiling ABC transporter genes in cancer cells. *Cancer Cell*. 2004; 6: 129–37.
57. **Türk D, Hall MD, Chu BF**, ***et al.*** Identification of compounds selectively killing multidrug-resistant cancer cells. *Cancer Res*. 2009; 69: 8293–301.
58. **Trompier D, Chang XB, Barattin R *et al.*** Verapamil and its derivative trigger apoptosis through glutathione extrusion by multidrug resistance protein MRP1. *Cancer Res*. 2004; 64: 4950–6.
59. **Efferth T, Giaisi M, Merling A**, ***et al.*** Artesunate induces ROS-mediated apoptosis in doxorubicin-resistant T leukemia cells. *PLoS One*. 2007; 2: e693.
60. **Michaelis M, Kleinschmidt MC, Barth S**, ***et al.*** Anti-cancer effects of artesunate in a panel of chemoresistant neuroblastoma cell lines. *Biochem Pharmacol*. 2010; 79: 130–6.
61. **Krungkrai SR, Yuthavong Y**. The antimalarial action on Plasmodium falciparum of qinghaosu and artesunate in combination with agents which modulate oxidant stress. *Trans R Soc Trop Med Hyg*. 1987; 81: 710–4.
62. **Lieschke GJ, Currie PD**. Animal models of human disease: zebrafish swim into view. *Nat Rev Genet*. 2007; 8: 353–67.
63. **Ingham PW**. The power of the zebrafish for disease analysis. *Hum Mol Genet*. 2009; 18: R107–12.

© 2011 The Authors
Journal of Cellular and Molecular Medicine © 2011 Foundation for Cellular and Molecular Medicine/Blackwell Publishing Ltd